Am J Physiol Heart Circ Physiol
281: H854–H864, 2001.

Pyruvate improves cerebral metabolism during hemorrhagic shock

PAUL D. MONGAN,[1] JOHN CAPACCHIONE,[1] JOHN L. FONTANA,[1]
SHANDA WEST,[1] AND ROLF BÜNGER[2]
[1]*Department of Anesthesiology and* [2]*Department of Physiology, Uniformed Services University of the Health Sciences, Bethesda, Maryland 20814*

Received 7 April 2000; accepted in final form 5 April 2001

Mongan, Paul D., John Capacchione, John L. Fontana, Shanda West, and Rolf Bünger. Pyruvate improves cerebral metabolism during hemorrhagic shock. *Am J Physiol Heart Circ Physiol* 281: H854–H864, 2001.—Pyruvate (PYR) improves cellular and organ function hypoxia and ischemia by stabilizing the reduced nicotinamide adenine dinucleotide redox state and cytosolic ATP phosphorylation potential. In this in vivo study, we evaluated the effects of intravenous pyruvate on neocortical function, indexes of the cytosolic redox state, cellular energy state, and ischemia during a prolonged (4 h) controlled arterial hemorrhage (40 mmHg) in swine. Thirty minutes after the onset of hemorrhagic shock, sodium PYR (n = 8) was infused (0.5 $g \cdot kg^{-1} \cdot h^{-1}$) to attain arterial levels of 5 mM. The volume and osmotic effects were matched with 10% NaCl [hypertonic saline (HTS)] (n = 8) or 0.9% NaCl [normal saline (NS)] (n = 8). During the hemorrhage protocol, the time to peak hemorrhage volume was significantly delayed in the PYR group compared with the HTS and NS groups (94 ± 5 vs. 73 ± 6 and 72 ± 4 min, $P < 0.05$). In addition to the early onset of the decompensatory phase of hemorrhagic shock, the complete return of the hemorrhage volume during decompensatory shock resulted in the death of five and four animals, respectively, in the HTS and NS groups. In contrast, in the PYR group, reinfusion of the hemorrhage volume was slower and all animals survived the 4-h hemorrhage protocol. During hemorrhage, the PYR group also exhibited improved cerebral cortical metabolic and function status. PYR slowed and reduced the rise in neocortical microdialysis levels of adenosine, inosine, and hypoxanthine and delayed the loss of cerebral cortical biopsy ATP and phosphocreatine content. This improvement in energetic status was evident in the improved preservation of the electrocorticogram in the PYR group. PYR also prevented the eightfold increase in the excitotoxic amino acid glutamate observed in the HTS group. The findings show that PYR administered after the onset of hemorrhagic shock markedly improves cerebral metabolic and functional status for at least 4 h.

microdialysis; glutamate; pyruvic acid

SINCE THE 1960s, early and aggressive fluid administration resuscitation has become the cornerstone of current trauma management. However, large volumes of resuscitation fluids can be associated with increased blood loss and poor outcome during uncontrolled hemorrhage. This is supported by both animal studies and a recent prospective study (2, 6, 42), in which survival was improved and morbidity decreased in trauma patients when resuscitation was delayed until definitive surgical treatment was available. Further work (6, 42) has shown that small volume resuscitation with moderate increases in blood pressure and O_2 delivery is more efficacious than aggressive resuscitation strategies. However, a system of rapid surgical stabilization and reversal of hemorrhagic hypotension is needed to restore organ perfusion and prevent multiple organ failure (3). Thus, in situations of delayed treatment, the risk of exacerbating hemorrhage must be balanced against inadequate tissue perfusion, tissue hypoxia, and ischemic injury that occur during severe hypotension. Whereas permissive hypotension during uncontrolled hemorrhage decreases blood loss, survival may not be enhanced due to the deleterious cerebral metabolic effects of prolonged hypotension (19, 29, 31). Therefore, a resuscitation solution that would enhance cellular function during volume-pressure-limited resuscitation regimens without an increase in blood loss would be of major benefit to trauma victims. Our initial study (34), targeted at enhancing cellular metabolic status during hemorrhagic hypotension, showed that the monocarboxylate pyruvate (PYR) administered before the onset of hemorrhagic shock, enhances cerebral O_2 consumption, delays the microdialysate rise in ATP breakdown product, and delays deterioration in the electrocortcogram (ECOG).

The current study expands on our previous work (34), which demonstrated that the administration of PYR before the onset of hemorrhagic shock improved the cerebral metabolic and functional status. However, the definitive interpretation of those results was limited by the study design, in which the hemorrhage volume (HV) was not reinfused and the animals were allowed to die during the decompensatory phase of hemorrhagic shock. Thus we were unable to determine if the differences in cerebral metabolic parameters were primarily related to the effects of PYR or differences in cerebral perfusion pressure. In the current

Address for reprint requests and other correspondence: P. Mongan, Dept. of Anesthesia, Uniformed Services Univ. of the Health Sciences, 4301 Jones Bridge Rd., Bethesda, MD 20814 (E-mail: pmongan@usuhs.mil).

The costs of publication of this article were defrayed in part by the payment of page charges. The article must therefore be hereby marked "*advertisement*" in accordance with 18 U.S.C. Section 1734 solely to indicate this fact.

study, we tested the hypothesis that PYR can improve cerebral metabolic status when it is administered after the onset of hemorrhagic shock. To evaluate this hypothesis, we implemented a computer-assisted hemorrhage system to maintain the mean arterial pressure (MAP) ~40 mmHg and simulated prolonged hypotensive hemorrhagic shock. The main parameters used to characterize the functional and metabolic status of the cerebral cortex were the following: *1*) the ECOG, *2*) microdialysate parameters of ATP catabolism and glutamate, *3*) cortical tissue content of phosphocreatine (PCr) and ATP, and *4*) the lactate-to-PYR (L/P) ratio of plasma and the microdialysate.

METHODS

Following Institutional Animal Care and Use Committee approval guidelines, 24 adolescent Yorkshire swine (*Sus scrofa*) were administered an intravenous infusion of either 30% PYR ($n = 8$), 10% NaCl [hypertonic saline (HTS), $n = 8$, osmotic control], or 0.9% NaCl [normal saline (NS), $n = 8$, volume control] 30 min after the start of controlled arterial hemorrhage. All animals were cared for according to the United States Department of Agriculture Animal Welfare Act and the National Institutes of Health *Guide for the Care and Use of Laboratory Animals*.

Animal Preparation and Monitoring

Anesthesia and hemodynamic monitoring procedures. Swine were fasted overnight but were given free access to water. In the morning, the swine were sedated with an intramuscular injection of ketamine (250 mg) and were anesthetized with halothane by nose cone to facilitate tracheal intubation. During surgical preparation, anesthesia was maintained with halothane (1.0% end-tidal concentration), while the animals spontaneously ventilated with a mixture of 25% O_2-75% N_2 through a semiclosed circle system (Narkomed 2B, North American Dräger; Telford, PA). Inspired and expired O_2, CO_2, and halothane concentrations were continuously monitored (model M1026A gas analyzer and model 68 clinical monitor, Hewlett-Packard; Andover, MA). The right external jugular vein was isolated, an 8.5-Fr introducer sheath was inserted, and a continuous thermodilution cardiac output pulmonary artery catheter was advanced through the sheath to measure pulmonary artery pressure and cardiac output (QVue, Abbott Critical Care; N. Chicago, IL). Both femoral arteries and a femoral vein were isolated and cannulated with 8.5-Fr introducer sheaths. A micromanometer (model MPC-500, Millar Instruments; Houston, TX) was inserted into the right femoral artery and advanced to the midthoracic aorta for the measurement of MAP. The second femoral artery sheath was used for controlled arterial hemorrhage and the femoral vein for infusions. Physiological data were displayed on an eight-channel clinical monitor (model 68, Hewlett-Packard), and the analog outputs were digitized and stored on a computer hard disk.

Craniectomy, ECOG, and microdialysis instrumentation. After hemodynamic instrumentation was performed, the swine were placed in the ventral recumbent position and the cranium was stabilized. The scalp and galea were reflected, and a wide craniectomy was performed (4 cm × 6 cm). Bilateral gold cup electrodes were placed on the surface of the dura ($Fp_{1,2}$ and $C_{3,4}$) for recording of a two-channel bipolar ECOG. The ECOGs were recorded (model 1000, Aspect; Natick, MA), filtered (1–30 Hz), digitized, and stored on a hard disk for review and analysis. Two microdialysis probes (model CMA-10, CMA/Microdialysis; Acton, MA) of concentric design (polycarbonate fiber length 4 mm, diameter 0.5 mm, 20,000 Dal molecular cutoff) were inserted 6 mm into the left frontal neocortex. The location of insertion was 1.5 cm left of the sagittal sinus and 2 and 2.5 cm anterior to the coronal suture. After the probes were inserted, the probes were perfused with artificial cerebrospinal fluid (155 mM Na^+, 1.1 mM Ca^{2+}, 0.83 mM Mg^{2+}, and 2.9 mM K^+, pH 7.4) at 2 μl/min using a precision multisyringe pump (model 102, CMA/Microdialysis) as previously described (34). Brain temperature was monitored by an epidural thermistor and intracranial pressure was monitored by a micromanometer (model MPC-500, Millar Instruments) inserted under the exposed dura.

Experimental Protocol

Computer-controlled arterial hemorrhage. One hour before hemorrhage was initiated, the expired halothane concentration was reduced to 0.8%, and the animals were allowed to spontaneously ventilate. Controlled arterial hemorrhage was automated to ensure reproducibility. In brief, a customized computer program (LabView version 5, National Instruments; Austin, TX) monitored the MAP. With the use of a proportional control feedback algorithm, the program controlled the speed and direction of a partial occlusion roller pump (MasterFlex Digital Console Drive, Cole-Parmer Instruments; Chicago, IL) that was connected to a femoral arterial cannula. At the start of the hemorrhage period, the computer program initiated blood withdrawal to decrease the MAP to 40 mmHg over 10 min. During hemorrhage, the blood was stored in a closed reservoir primed with sodium citrate (1.66 g) and porcine heparin (3,000 U) to inhibit clot formation. After the initial 10-min rapid hemorrhage ended, the program maintained the MAP at 40 mmHg either by withdrawal or by reinfusion of the hemorrhage blood as necessary. During the protocol, the volume in the reservoir was gravimetrically measured (model LA4200, Sartorius; Edgewood, NY) and the data output stored on computer hard disk with the time-stamped MAP. With the exception of the protocol infusions of PYR, HTS, or NS, only the blood withdrawn to induce hypotension was administered to maintain the MAP at 40 mmHg. During the decompensatory phase of hemorrhagic shock, if all of the hemorrhage volume was reinfused, no further therapy was used to support the MAP. Death was defined as a MAP <10 mmHg with cessation of spontaneous respiratory effort.

PYR and HTS infusion protocols. The animals were administered one of three treatments. *Group 1* was administered a 100 mg/kg bolus of 30% sodium pyruvate (pH titrated to 7.4 with 1 N NaOH) via the femoral vein, followed by 0.5 $g \cdot kg^{-1} \cdot h^{-1}$ for the duration of the protocol. To control for the volume and osmolarity effects of the HTS pyruvate, *group 2* was administered an equivalent volume of HTS, and *group 3* an equivalent volume of NS.

Analytical sampling procedures. Microdialysis samples were continuously collected over 30-min periods (60-μl aliquots) by an automated microfraction collector (model CMA142, CMA/Microdialysis). All analytical tests were performed within 12 h (lactate, PYR, and glutamate, followed by high-performance liquid chromatography analysis for ATP degradation products). One hour after the microdialysis probes were inserted, arterial blood was sampled every 30 min for measurement of pH, base excess, blood gases, and hemoglobin content (models IL 1610 and IL 682 CoOx, Instrumentation Laboratories; Lexington, KY). Heparinized

blood samples for electrolytes (Na, K, Cl, and HCO_3), osmolality, lactate, and PYR were obtained every 30 min and were immediately centrifuged.

Cerebral cortical tissue sampling. Tissue samples were obtained from the cerebral cortex immediately before and 60 and 120 min after the start of the hemorrhage protocol (H_0, H_{60}, and H_{120}). To ensure that cerebral cortical tissue was obtained at similar perfusion pressures, the final biopsy (H_{final}) was made at the end of the protocol (H_{240}) or at the completion of the HV reinfusion if it occurred before H_{240}. For the cerebral cortical biopsies, a small incision in the dura was made. In general, the cortical biopsy sites were from gyri located 1 cm lateral to the sagittal sinus and 1.5 cm anterior or posterior to the coronal suture with minor adjustments as necessary to avoid cortical vessels. With the use of these references, the cortical biopsies were taken in order from right anterior (H_0), right posterior (H_{60}), left posterior (H_{120}), and finally left anterior (H_{final}) adjacent to the microdialysis probes. Biopsies were performed with 8-mm cortical biopsy forceps that were precooled to 0°C. The cortical biopsies (≈100 mg each) were rapidly immersed (<0.5 s) in liquid isopentane at ≤80°C. After the biopsy was completed, cortical bleeding was controlled with a thrombin and collagen matrix. After the tissue was frozen, it was transferred to cryovials chilled with liquid nitrogen and was stored at −80°C for future analysis.

Analytical Methods

ATP, PCr, and creatine analysis of cerebral cortical tissue. Cortical tissue biopsies were transferred from storage to a cooling device (−20°C; Polar Block II, Boekel Scientific; Feasterville, PA) and homogenized with ice-cold perchloric acid (0.5 ml, 0.6 N) by using a tissue tearor (Biospec Products; Racine, WI). After the tissues were homogenized, the samples were centrifuged at 15,000 *g* for 10 min at −4°C, and the supernatant was decanted and neutralized with 0.2 ml 1 N KOH and $KHCO_3$ for a final pH of 6.5–7.0 at −4°C. After 20 min, the $KCLO_4$ precipitate was removed by centrifugation (−4°C), and an aliquot of the extract was assayed for ATP, PCr, and creatine by enzymatic spectrophotometric methods.

Microdialysis calibration procedures. In vitro relative recovery for each microdialysis probe was determined in triplicate before and after each experiment. In brief, the probes were immersed in a calibration standard solution at 38.5°C and perfused with artificial cerebrospinal fluid (34). The calibration standards contained hypoxanthine (HX; 10 μM), insosine (Ino; 10 μM), adenosine (Ado;10 μM), glutamate (10 μM), lactate (10 mM), and PYR (2 mM) in double-distilled deionized water. The concentrations of the nondialyzed standards were compared with the concentrations of the in vitro microdialysis samples to determine the relative recovery for each component. The relative recovery for each compound was used to estimate the in vivo extracellular concentration of the components in the immediate vicinity of the probes.

Lactate, PYR, and glutamate analysis. Lactate and PYR were measured in serum samples and the microdialysate. In addition, the microdialysis samples were also analyzed for glutamate content by using an analyzer (model 600, CMA/Microdialysis). In brief, the analyzer enzymatically converts lactate, PYR, and glutamate to H_2O_2 peroxidase catalyses, a reaction between H_2O_2 and other substrates to form the red-violet-colored quinonediimine. The rate of formation of the quinonediimine is measured at 546 nm and is proportional to the lactate, PYR, and glutamate concentrations.

High-performance liquid chromatography analysis of purines. Analysis of HX, Ino, and Ado in the microdialysate was performed by using a photodiode array reverse phase high-performance liquid chromatography technique (34). In brief, neocortical microdialysis samples (30 μl) were automatically injected into a heated C-18 column (30°C) by a refrigerated (4°C) autosampler (model 2690 separation module; Waters Associates; Milford, MA). Chromatograms and absorbance data from the photodiode array (model 996, Waters Associates) were recorded and analyzed with the use of Millenium 32 software (Waters Associates). Peak identification and quantification were accomplished by matching the spectral signal of the peaks, peak purity, and peak areas to the spectral signal, and peak areas generated for the injected standards.

ECOG analysis. The ECOG was analyzed using a five-point visual scale previously reported (34). The 10-s ECOG epochs from each measurement period were reviewed by an investigator blinded to animal treatment status. The ECOG was assigned a numeric score: 5, unchanged from baseline; 4, mildly depressed (25%) amplitude and frequency compared with baseline; 3, moderate depression (50%) of amplitude and frequency from baseline; 2, markedly depressed (75%) amplitude and frequency from baseline; and 1, burst suppression or an isoelectric ECOG.

Data Presentation and Statistics

All data are presented as means ± SE or median with range in the text, tables, and figures. Differences among the groups for nonrecurring measurements were assessed with the use of analysis of variance. Differences among and within groups over the course of the experiment were determined by analysis of variance among groups for the dependent variable (i.e., MAP and cerebral blood flow) with repeated measures over time. Within- and among-groups testing was accompanied by Tukey's honestly significant difference multiple-range test to correct for multiple comparisons. Nonparametric analysis was performed on the ECOG data. Values were considered statistically different when $P < 0.05$ after correction for multiple comparisons.

RESULTS

The animal weights in the PYR, HTS, and NS groups were similar: 32.0 ± 0.7, 31.6 ± 0.8, and 31.8 ± 1.1 kg, respectively. Thirty minutes after the start of controlled arterial hemorrhage, the bolus and infusion of PYR raised the arterial PYR concentration from 0.09 ± 0.01 mM at H_{30} to 4.58 ± 0.83 mM at H_{60} (Fig. 1). In the HTS and NS groups, the PYR levels at H_{30} were 0.11 ± 0.02 and 0.08 ± 0.01 mM and rose to only 0.39 ± 0.03 and 0.38 ± 0.02 mM during hemorrhage (Fig. 1).

Hemorrhage Model and Physiological Parameters

Table 1 and Fig. 2 show the accuracy and precision of our automated hemorrhage system for the induction and maintenance of the target MAP of 40 mmHg. In addition, the intradural pressure, and thus the cerebral perfusion pressure, were similar in all groups before and during the experiment (Table 1). Figure 2 also displays the accumulation and reinfusion of the hemorrhage volume (HV) during the controlled arterial hemorrhage protocol. There was no significant difference in the peak HV (45.7 ± 1.5 vs. 41.9 ± 2.1 ml/kg)

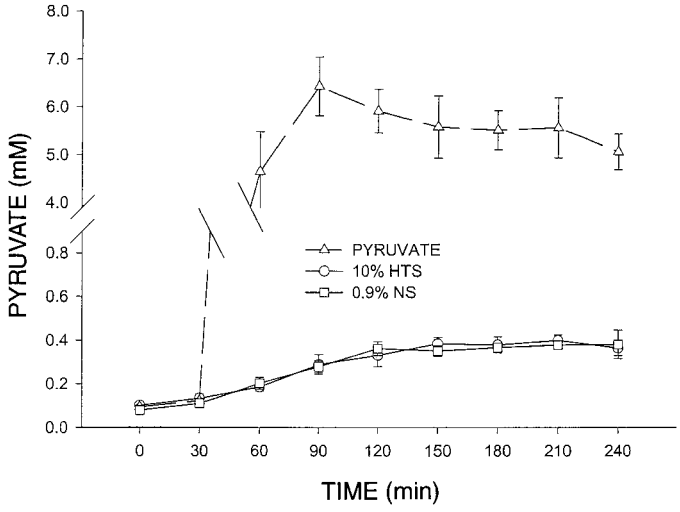

Fig. 1. Arterial pyruvate (PYR) levels (means ± SE) before and during controlled hemorrhage. PYR was infused (100 mg/kg, followed by 0.5 $g \cdot kg^{-1} \cdot h^{-1}$) starting 30 min after the onset of the hemorrhage protocol. Control groups were administered either 10% hypertonic NaCl [10% hypertonic saline (HTS)] or 0.9% isotonic NaCl [0.9% normal saline (NS)] to control for the volume, sodium, and osmotic effects.

between the PYR and HTS treatments. However, the peak HV was significantly lower in the NS group 37.8 ± 1.8 ml/kg ($P < 0.05$). This difference is attributed to the mobilization of extravascular water to expand and reconstitute the intravascular volume. More importantly, the PYR treatment was more effective in delaying cardiovascular decompensation as evidenced by the increased time to the peak HV (PHV; 94 ± 5 vs. 73 ± 6 and 72 ± 4 min, $P < 0.05$). The beneficial effects of PYR during the decompensatory phase of hemorrhagic shock are evident in the decrease in HV return (Fig. 2, Table 1) and the cardiovascular profiles during the last hours of the hemorrhage. After H_{150}, the HTS and NS groups were unable to increase their cardiac index (CI), despite continued infusion of the HV with increases in the CVP. This inability to augment the CI to help maintain the MAP resulted in complete reinfusion of the HV, cardiovascular collapse, and death in five of the eight HTS and four of the eight NS animals. In contrast, despite the smaller amount of HV return, the PYR-treated animals suffered no animal deaths throughout the protocol. Table 2 details changes in laboratory measurements including the systemic L/P ratio. The increases in osmolarity and decreases in hemoglobin during the protocol were similar in the PYR and HTS groups and significantly different from

Table 1. *HV and physiological measurements*

Variable	Time, min								
	H_0	H_{30}	H_{60}	H_{90}	H_{120}	H_{150}	H_{180}	H_{210}	H_{240}
Surviving animals									
Pyruvate	8	8	8	8	8	8	8	8	8
HTS	8	8	8	8	8	7	6	5	3
NS	8	8	8	8	8	7	6	5	4
HV, ml/kg									
Pyruvate	0	25.6 ± 2.3	42.2 ± 2.9	44.7 ± 2.6	41.6 ± 3.3	35.7 ± 2.3	25.9 ± 3.0	22.2 ± 3.3	14.9 ± 3.7
HTS	0	26.0 ± 1.5	39.5 ± 1.2	38.8 ± 2.0	34.3 ± 2.3	26.3 ± 2.1*	16.2 ± 2.9*	5.5 ± 2.1*	2.6 ± 1.3*
NS	0	25.7 ± 1.2	36.6 ± 1.0	34.2 ± 1.4*	30.3 ± 1.3*	22.1 ± 2.1*	14.8 ± 3.8*	9.3 ± 4.2*	3.8 ± 2.3*
MAP, mmHg									
Pyruvate	97.1 ± 3.1	39.8 ± 0.2	39.9 ± 0.1	40.0 ± 0.2	39.8 ± 0.4	39.6 ± 0.2	39.5 ± 0.3	38.8 ± 1.4	38.1 ± 1.2
HTS	101.9 ± 3.2	40.1 ± 0.1	39.8 ± 0.2	38.4 ± 1.3	39.5 ± 0.4	39.6 ± 0.4	38.6 ± 0.9	37.5 ± 4.1	20.0 ± 9.9*
NS	100.9 ± 2.4	40.3 ± 0.2	40.3 ± 02	39.8 ± 0.2	38.6 ± 0.9	38.9 ± 0.9	38.8 ± 0.9	38.6 ± 0.7	32.0 ± 2.7
CVP, mmHg									
Pyruvate	1.0 ± 0.9	−5.6 ± 0.7	−6.0 ± 0.8	−6.9 ± 0.9	−6.8 ± 0.8	−5.5 ± 0.7	−5.2 ± 0.6	−5.5 ± 0.7	−4.8 ± 0.6
HTS	1.5 ± 0.6	−5.9 ± 0.8	−6.4 ± 0.6	−6.5 ± 0.5	−5.6 ± 0.6	−5.1 ± 0.5	−4.3 ± 0.6	−4.3 ± 0.7	−3.9 ± 1.2
NS	1.4 ± 0.6	−5.8 ± 0.6	−5.8 ± 0.9	−6.5 ± 0.8	−5.9 ± 1.2	−5.0 ± 0.8	−4.6 ± 1.0	−3.8 ± 1.2	−3.4 ± 1.3
IDP, mmHg									
Pyruvate	5.4 ± 0.7	0.8 ± 0.2	0.8 ± 0.2	0.6 ± 0.2	0.8 ± 0.2	0.7 ± 0.2	0.8 ± 0.1	0.9 ± 0.2	0.8 ± 0.2
HTS	5.2 ± 09	1.0 ± 0.3	0.9 ± 0.3	0.8 ± 0.2	0.7 ± 0.3	0.8 ± 0.1	0.9 ± 0.2	0.7 ± 0.2	1.0 ± 0.2
NS	4.8 ± 0.8	1.1 ± 0.2	0.8 ± 0.2	0.7 ± 0.3	0.8 ± 0.2	0.9 ± 0.3	0.8 ± 0.1	0.9 ± 0.1	0.9 ± 0.2
CI, $ml \cdot kg^{-1} \cdot min^{-1}$									
Pyruvate	174.7 ± 13.3	66.3 ± 6.7	46.9 ± 4.5	40.2 ± 3.8	46.1 ± 3.1	53.2 ± 3.9	60.5 ± 3.9	67.4 ± 5.4	71.2 ± 4.1
HTS	167.1 ± 13.5	61.6 ± 4.2	46.4 ± 4.2	37.1 ± 3.1	38.1 ± 2.5	45.4 ± 3.8	45.1 ± 4.9	43.9 ± 3.5*	47.3 ± 5.1*
NS	189.5 ± 8.5	68.4 ± 3.2	51.4 ± 3.9	39.5 ± 4.4	42.5 ± 4.8	46.4 ± 5.3	46.6 ± 5.3	47.5 ± 4.3*	48.5 ± 4.2*
Temperature, °C									
Pyruvate	38.3 ± 0.1	38.6 ± 0.1	39.0 ± 0.2	39.0 ± 0.2	38.9 ± 0.2	38.8 ± 0.3	38.8 ± 0.3	39.0 ± 0.3	38.7 ± 0.3
HTS	38.3 ± 0.1	38.5 ± 0.1	39.1 ± 0.1	39.0 ± 0.1	38.9 ± 0.1	39.0 ± 0.1	39.0 ± 0.1	39.1 ± 0.2	39.0 ± 0.2
NS	38.4 ± 0.1	38.5 ± 0.1	39.0 ± 0.1	38.9 ± 0.2	38.8 ± 0.1	38.9 ± 0.2	38.9 ± 0.2	38.9 ± 0.1	38.8 ± 02

Values are means ± SE. HV, hemorrhage volume; MAP, mean arterial pressure; CVP, central venous pressure; IDP, intradural pressure; HTS, 10% NaCl treatment; NS, 0.9% NaCl treatment; and CI, cardiac index. Initial hemodynamic measurements were made before the start of the controlled arterial hemorrhage (H). Pyruvate (10%) or the 0.9% NaCl treatments were started at H_{30}, which was 30 min after the start of hemorrhage. *$P < 0.05$ compared with the pyruvate group for the time-matched data.

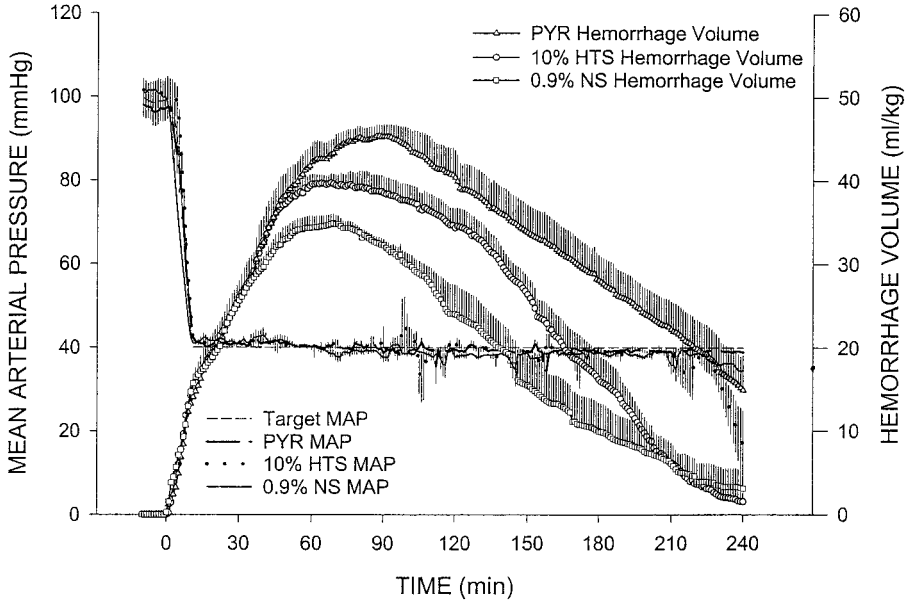

Fig. 2. A computerized hemorrhage system provided tight and equivalent control of blood withdrawal before the start of the PYR, 10% HTS, and 0.9% NS infusions. Mean arterial pressure (MAP) was controlled throughout the protocol by continued blood withdrawal until the peak hemorrhage volume (PHV) was reached. After PHV was attained, blood was returned to support MAP. When no autologous blood was available for infusion, the animals were allowed to spontaneously decompensate and die. Although there was no significant difference in the PHV in the PYR and 10% HTS groups (45.7 ± 1.5 vs. 41.9 ± 2.1 ml/kg, respectively), the PHV was significantly lower in the NS group (37.8 ± 1.8 ml/kg; $P < 0.05$). More importantly, there was also a delay in the time to reach the PHV in the PYR group (94.5 ± 5 vs. 73 ± 6 min, and 72 ± 4 min, $P < 0.05$). In addition to the delay in PHV, the rate of reinfusion was slower in the PYR group. This difference resulted in complete HV infusion and death in 5 animals in the HTS group and 4 in the NS group compared with 100% survival in the PYR group.

the volume infusion of the NS alone. These data, in conjunction with the similar CVPs and slower HV return, indicate the PYR effects were not related to volume or osmotic effects alone. The laboratory data also indicate that the severity of hemorrhage before the start of therapy was similar due to similar increases in lactate and L/P ratio and decreases in base excess 30 min after the start of hemorrhage (Table 2). However,

Table 2. *Osmolality, hemoglobin, lactate, and acid-base status*

Variable	Time, min								
	H_0	H_{30}	H_{60}	H_{90}	H_{120}	H_{150}	H_{180}	H_{210}	H_{240}
No. of swine									
Pyruvate	8	8	8	8	8	8	8	8	8
HTS	8	8	8	8	8	7	6	5	3
NS	8	8	8	8	8	7	6	5	4
Osmolarity, meq/l									
Pyruvate	271 ± 3	269 ± 4	296 ± 4	309 ± 5	310 ± 4	315 ± 5	319 ± 4	322 ± 5	327 ± 5
HTS	268 ± 4	269 ± 2	300 ± 5	309 ± 4	309 ± 3	318 ± 5	320 ± 5	327 ± 10	329 ± 7
NS	268 ± 3	267 ± 3	267 ± 3*	267 ± 2*	267 ± 3*	268 ± 3*	270 ± 3*	270 ± 3*	269 ± 5*
Hemoglobin, g/dl									
Pyruvate	9.4 ± 0.2	8.5 ± 0.1	7.4 ± 0.3	6.6 ± 0.2	7.0 ± 0.1	7.0 ± 0.2	7.1 ± 0.2	7.2 ± 0.4	7.2 ± 0.4
HTS	9.2 ± 0.1	8.3 ± 0.2	7.4 ± 0.2	6.6 ± 0.2	6.8 ± 0.2	6.9 ± 0.2	7.0 ± 0.3	7.3 ± 0.4	7.7 ± 0.4
NS	9.5 ± 0.1	8.4 ± 0.2	8.8 ± 0.2*	9.1 ± 0.3*†	9.6 ± 0.4*†	9.7 ± 0.4*†	9.7 ± 0.5*†	9.8 ± 0.4*†	9.8 ± 0.3*†
Lactate, mM									
Pyruvate	1.2 ± 0.2	3.0 ± 0.2	11.3 ± 1.9	20.9 ± 1.0	27.6 ± 1.7	28.2 ± 0.9	29.6 ± 0.9	30.7 ± 0.9	30.9 ± 1.3
HTS	1.2 ± 0.1	3.3 ± 0.3	6.7 ± 1.1*	11.5 ± 1.4*	13.7 ± 1.4*	14.7 ± 1.2*	14.8 ± 0.9*	15.0 ± 1.1*	13.9 ± 1.3*
NS	1.2 ± 0.2	3.1 ± 0.4	6.8 ± 1.2*	11.0 ± 1.0*	11.6 ± 0.9*	12.1 ± 0.8*	13.6 ± 0.7*	14.4 ± 0.8*	12.3 ± 1.1*
Lactate/pyruvate									
Pyruvate	12.2 ± 1.2	27.1 ± 4.6	4.8 ± 0.5	3.4 ± 0.3	4.9 ± 0.5	4.9 ± 0.4	5.5 ± 0.3	6.0 ± 0.7	6.3 ± 0.6
HTS	12.3 ± 1.5	28.4 ± 4.5	36.3 ± 4.8*	41.5 ± 3.4*	43.9 ± 3.3*	38.5 ± 2.2*	40.3 ± 2.7*	37.6 ± 2.3*	38.3 ± 2.3*
NS	13.4 ± 1.2	25.7 ± 3.2	33.2 ± 2.3*	33.9 ± 2.6*	35.2 ± 3.1*	34.1 ± 2.9*	33.7 ± 2.2*	33.2 ± 1.8*	33.8 ± 1.9*
Base excess, meq/l									
Pyruvate	3.6 ± 0.8	−1.5 ± 0.2	−0.8 ± 1.2	−2.0 ± 2.1	−2.2 ± 2.2	−1.2 ± 2.2	0.5 ± 3.0	5.4 ± 3.3	5.0 ± 4.4
HTS	3.5 ± 0.9	−1.2 ± 0.8	−6.2 ± 1.9*	−11.3 ± 2.1*	−13.5 ± 2.0*	−17.0 ± 1.2*	−16.9 ± 1.0*	−17.2 ± 1.5*	−13.7 ± 3.1*
NS	4.1 ± 0.9	−0.8 ± 0.4	−5.8 ± 1.2	−10.5 ± 1.7*	−11.6 ± 1.2*	−13.8 ± 1.5*	−14.7 ± 1.4*	−14.9 ± 1.3*	−14.1 ± 2.6*
pH									
Pyruvate	7.42 ± 0.01	7.38 ± 0.02	7.36 ± 0.04	7.39 ± 0.05	7.40 ± 0.05	7.38 ± 0.05	7.39 ± 0.04	7.41 ± 0.04	7.39 ± 0.04
HTS	7.42 ± 0.01	7.42 ± 0.01	7.34 ± 0.03	7.24 ± 0.03*	7.16 ± 0.04*	7.08 ± 0.03*	7.04 ± 0.03*	7.12 ± 0.06*	7.13 ± 0.09*
NS	7.41 ± 0.01	7.41 ± 0.01	7.37 ± 0.03	7.25 ± 0.02*	7.23 ± 0.05*	7.21 ± 0.03*	7.18 ± 0.05*	7.17 ± 0.05*	7.18 ± 0.06*

Values are means ± SE. Initial measurements were made immediately before the start of the controlled arterial hemorrhage. Pyruvate (10%) or the 0.9% saline treatments were started at H_{30}. *$P < 0.05$ compared with the pyruvate group for the time-matched data. †$P < 0.05$, compared with the HTS group for time-matched data.

Table 3. *Effects of pyruvate on cerebral cortical tissue energy metabolites*

Variable	Time, min			
	H_0	H_{60}	H_{120}	H_{final}
No. of swine				
Pyruvate	8	8	8	8
HTS	8	8	8	8
NS	8	8	8	7
ATP, μmol/g dry wt				
Pyruvate	16.4 ± 2.1	17.4 ± 2.8	18.9 ± 0.8	8.5 ± 2.4
HTS	17.6 ± 1.8	11.5 ± 1.7	8.5 ± 1.8*	2.9 ± 0.9*
NS	16.6 ± 1.3	11.6 ± 0.9	9.2 ± 1.5*	2.8 ± 0.4*
Phosphocreatine, μmol/g dry wt				
Pyruvate	11.9 ± 0.9	9.7 ± 0.9	11.2 ± 0.8	3.9 ± 1.3
HTS	12.3 ± 2.2	4.9 ± 0.8*	3.4 ± 1.3*	2.8 ± 1.1
NS	11.1 ± 1.8	6.2 ± 0.7*	3.2 ± 0.8*	1.2 ± 0.9
Creatine, μmol/g dry wt				
Pyruvate	43.3 ± 2.8	47.0 ± 2.1	46.8 ± 2.8	58.1 ± 2.4
HTS	45.7 ± 2.4	54.4 ± 2.8	56.6 ± 2.2*	55.9 ± 3.4
NS	46.1 ± 2.7	51.2 ± 3.4	59.9 ± 3.4*	60.5 ± 2.6

Values are means ± SE. Initial cortical tissue biopsies were made immediately before the start of the controlled arterial hemorrhage. Pyruvate (10%) or 0.9% NaCl treatments were started at H_{30}. Final biopsies (H_{final}) were obtained 240 min after the start of hemorrhage if the animal did not require complete infusion of the HV to maintain a MAP of 40 mmHg. If all of the HV was infused before 240 min, the biopsy was obtained at that time to ensure equivalent perfusion pressures in all animals at the time of biopsy. *$P < 0.05$ compared to the pyruvate group for the time matched data (ANOVA).

after the initiation of the PYR, HTS, and NS treatments, there were significant differences in laboratory parameters among the groups for the remainder of the protocol. In the HTS and NS groups there were continued significant increases in lactate and the L/P ratio and decreases in base excess and pH. In comparison, although the PYR treatment caused lactate to increase two times higher than the other groups, the L/P ratio, a more relevant indicator of metabolic redox status and stress, was decreased to one-half of the initial value. These data indicate that the delay in decompensation and improved cardiovascular status by PYR was not due to the potential deleterious effects of HTS on the acid base status of the animals.

PYR Effects on High-Energy Phosphates of Cerebral Cortical Biopsies

Table 3 details the differences among the groups for the cerebral cortical high-energy phosphate indices as judged by the ATP, PCr, and creatine contents measured in the cerebral cortical biopsies. The basal levels of ATP, PCr, and creatine before hemorrhage (H_0) were similar for both groups. During the hemorrhage protocol, these parameters remained at the basal levels for the first 120 min of hemorrhage in the PYR group suggesting energetic stability of the cerebral cortex. In contrast, the animals administered HTS or NS demonstrated a marked catabolic profile as indicated by the progressive decline in ATP and PCr content with a concomitant rise in creatine. Whereas the results from the final biopsies revealed similar PCr and creatine content for all groups, there was still a marked difference in the ATP content. In the PYR animals, the ATP content was still 50% of the basal level. This was threefold higher than in the HTS or NS groups (8.5 ± 2.4 μmol/g dry wt vs. 2.9 ± 0.9 and 2.8 ± 0.04 μmol/g dry wt, $P < 0.05$) and suggests substantial preservation of the energetic status.

PYR Effects on Cortical Microdialysate Adenosine Purines, L/P ratio, and Glutamate

Figures 3 and 4 illustrate the cerebral cortical metabolic differences among the treatment groups in terms of the ATP adenylate breakdown products (HX + Ino + Ado), the L/P ratio, and glutamate accumulation. These indexes of cortical energetics (adenosine purines), redox status (L/P ratio), and neuronal metabolic failure (glutamate) were measured in the microdialysates. Figure 3*A* shows that 30 min after the start of the PYR treatment (H_{60}), there was both a delay and

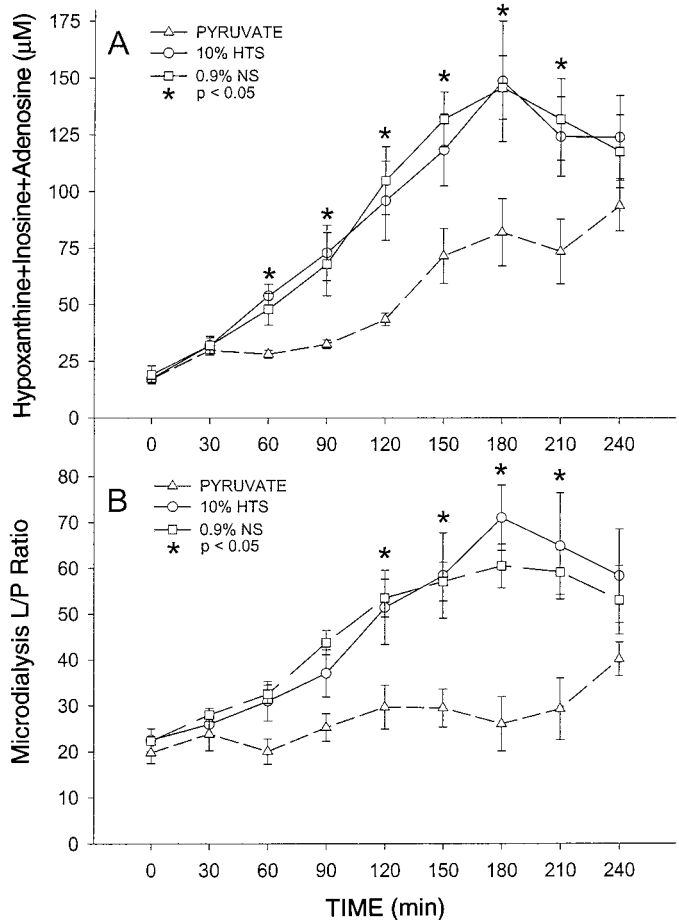

Fig. 3. *A*: microdialysis accumulation of the adenylate end products of ATP catabolism. Administration of PYR had a significant effect in delaying and attenuating the rise in these parameters indicating significant stabilization of the cerebral cortical energetics. *B*: changes in the microdialysis lactate-to-PYR (L/P) ratio during the protocol. Increases in the 10% HTS- and 0.9% NS-treated animals were due to a rapid and significant increase in lactate.

attenuation of the accumulation of the adenylate catabolites, Ado, Ino, and HX, which persisted throughout the protocol. This finding is consistent with the apparent stability of the cortical biopsy ATP content in this group (Table 4). Figure 3*B* shows the results for the microdialysate L/P ratio measurements. The lactate, PYR, and L/P ratio were similar in all groups before (H_0) and 30 min after the start of hemorrhage (H_{30}, before treatment). However, the PYR infusion increased the microdialysate PYR levels from 0.09 to 0.43 mM during the experiment compared with the increases from 0.10 and 0.08 to 0.13 and 0.12 mM in the HTS and NS animals, respectively ($P < 0.05$). Compared with the HTS and NS control groups, this rise in PYR resulted in a significantly lower and more stable L/P ratio until near the end of the protocol (H_{240}). Associated with the delayed decrease in ATP and PCr contents and the attenuated rise of the microdialysis adenosine purines in the PYR group was the marked delay in microdialysis accumulation of the excitotoxic amino acid glutamate (Fig. 4). Taken together, these data suggest significantly improved cerebral cortical metabolic and energetic status and ischemic tolerance throughout the protocol secondary to the administration of PYR (5 mM; Fig. 1).

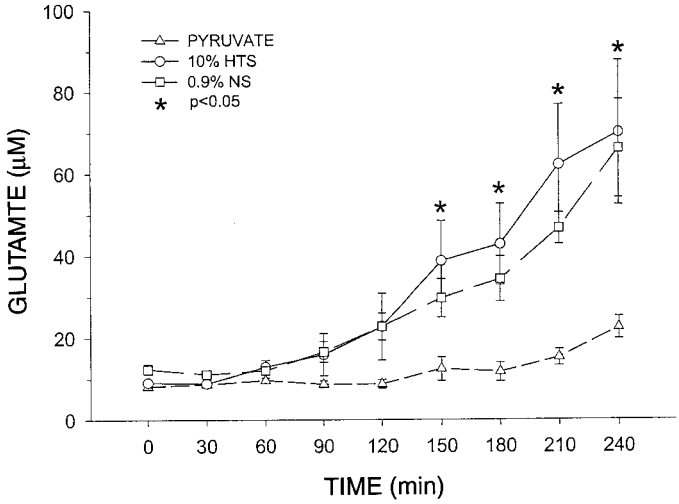

Fig. 4. Microdialysis accumulation of the excitatory amino acid glutamate for the PYR-, 10% HTS-, and 0.9% NS-treated animals. Levels of glutamate were significantly higher in the 10% HTS and 0.9% NS groups from 150 min after the start of hemorrhage until the end of the experiment.

Table 4. *Electrocorticogram scores*

	Visual Score		
Time, min	Pyruvate	HTS	NS
H_0			
Median	5	5	5
Range	5	5	5
N	8	8	8
H_{30}			
Median	4	4	4
Range	3–5	3–5	3–5
N	8	8	8
H_{60}			
Median	3.5	3.5	3.5
Range	3–5	3–4	3–4
N	8	8	8
H_{90}			
Median	3.5	3	3
Range	3–4	3–4	3–4
N	8	8	8
H_{120}			
Median	3	2.5*	2.5*
Range	3–4	2–3	2–3
N	8	8	8
H_{150}			
Median	3.5	3*	2*
Range	3–4	2–3	2–3
N	8	7	7
H_{180}			
Median	3	2*	2*
Range	2–3	2–3	2–3
N	8	6	6
H_{210}			
Median	3	2*	2*
Range	2–3	2	1–2
N	8	5	5
H_{240}			
Median	3	2*	1.5*
Range	2–3	2	1–2
N	8	3	4

Values are presented as the median with range. H_0 was immediately before the initiation of hemorrhage (H). Changes in the electrocorticograms (ECOG) from baseline were graded using a 5-point visual scale. Ten-second ECOG epochs recorded at the end of each measurement period were reviewed by an investigator blinded to animal treatment as detailed in METHODS. *$P < 0.05$ compared with the pyruvate group for the time-matched data.

PYR Effects on Cerebral Cortical Electrophysiological Status

Table 4 summarizes the results from the ECOG data analysis. The ECOG scores were consistently higher in the PYR group than in the HTS group for the final 2 h of the hemorrhagic shock protocol. These data indicate that despite the severe decreases in cerebral perfusion pressure induced by the hemorrhagic hypotension, PYR administration prevented neuronal deenergization, maintained electrical function (ECOG), and cellular membrane integrity (decreased glutamate release).

DISCUSSION

The primary findings in the present study are that PYR (5 mM) administered 30 min after the start of rapid severe controlled arterial hemorrhage in swine preserved cerebral cortical metabolic, energetic, and functional status as indicated by a delay and attenuation in *1*) the microdialysate rise in ATP breakdown products, *2*) cortical tissue ATP and PCr depletion, *3*) the deterioration in the ECOG, and *4*) prevention of major release of the excitatory amino acid, glutamate. These results are consistent with the findings of our previous study in which PYR was administered before the onset of hemorrhagic shock and support the hypothesis that the administration of appropriate metabolically active substrates has the potential to attenuate the deleterious effects of hypotension during severe hemorrhagic shock.

Automated Isobaric Controlled Arterial Hemorrhage Model

There are numerous models, both controlled and uncontrolled, for inducing experimental hemorrhagic shock. The controlled isobaric model attempts to maintain the hemorrhage pressure at a set point and uses blood withdrawal during compensated shock or reinfusion during the decompensatory phase to achieve that goal. In our previous study (34) of PYR during controlled arterial hemorrhage at 40 mmHg, we did not intervene to support the MAP because we intended to evaluate the efficacy and mechanism of PYR in delaying death during the decompensatory phase of hemorrhagic shock. In that study, it was evident that spontaneous loss of vascular tone resulted in a decrease in the MAP. The decrease in perfusion pressure caused severe cerebral and cardiac dysfunction leading to the death of the animals. In addition to PYR delaying the onset of spontaneous vascular decompensation, the data suggested that cerebral metabolic and functional status was also improved by PYR. However, because of the differences in the time to vascular decompensation, the cerebral perfusion pressure was different among groups at the measurement times, and the data suggested but did not conclusively support an improvement in cerebral metabolic status. Because this investigation is primarily focused on the ischemic metabolic changes that occur during hemorrhage, we eliminated the confounding variable of perfusion pressure during the untreated decompensatory phase of hemorrhage by implementing an automated isobaric controlled arterial hemorrhage and reinfusion system to maintain the MAP at 40 mmHg for 4 h. This computerized application of the isobaric controlled arterial hemorrhage model allows for extended control of the critical variable of perfusion pressure with minimal investigator intervention. In brief, the custom virtual instrument created in Labview monitors the difference in the target and actual MAP. By using a proportional feedback control algorithm, the program automatically controls the speed and direction of the pump to minimize the difference in the target and actual MAP. The present data (Fig. 1) demonstrate that the system is capable of tight control of the hemorrhage protocol with minimal variability in reaching and maintaining the target MAP. Because of this tight control of the MAP, the cerebral perfusion pressure was virtually constant throughout the experiment (Table 1).

PYR Improvement in Cerebral Energy Parameters

In the current study, the animals administered the HTS (10% NaCl) and NS (0.9% NaCl) controls exhibited significant neocortical deenergization during the 4-h controlled arterial hemorrhage protocol. During hypotension, the microdialysis data from that group shows a rapid increase in the dialysate and, hence, interstitial Ado, Ido, and HX (Fig. 3*A*). These parameters reflect substantial neocortical ATP degradation and are predictive of poor outcome (14, 28, 44). In addition, the microdialysis accumulation of cortical ATP degradation products was mirrored in the progressive decline in cerebral biopsy high-energy phosphate content (ATP and PCr; see Table 3) and massive accumulation of creatine over the 4-h protocol. In marked contrast, in the PYR animals the cerebral energetic parameters were strikingly improved during the severe prolonged hemorrhagic hypotension. At 4 h, the cerebral biopsy ATP was still ~50% of control and the depletion of the PCr pool was attenuated for more than 2 h (Table 3). This was associated with both a delay and attenuation in the dialysate purine accumulation (Fig. 3*A*). The improved high-energy phosphate stability and reduced rate of ATP catabolism was associated with increased cortical PYR availability. In the PYR animals, the microdialysate PYR levels were increased 2.5 times (0.09 ± 0.03 to 0.43 ± 0.02 mM) compared with minimal rise in the HTS and NS control groups (Fig. 1). This indicates that the intravenous PYR was able to cross the blood-brain barrier during hemorrhage and markedly helped stabilize the cerebral neocortical energetics.

Because the critical variables of cerebral temperature and perfusion pressure (Table 1) were closely controlled, it is evident that the PYR had a substantial metabolic enhancing effect that resulted in the attenuation in release of the toxic excitatory amino acid, glutamate (Fig. 4), and the delayed deterioration in the indicator of electrophysiologic function, the ECOG (Table 4). In the PYR-treated animals, compared with the basal levels, there was a virtual absence of dialysis glutamate accumulation despite the prolonged severe hypotension. This was in stark contrast to the approximate eightfold accumulation of this excitotoxic amino acid in the HTS and NS controls (Fig. 4). The improvement in energetic and neuronal metabolic conditions in the PYR animals during shock was also reflected in the ECOG scores. In the PYR-treated animals, decreases in ECOG activity were limited to 50%, whereas there was a 75–100% decrease in ECOG activity in many of the HTS and NS-treated animals (Table 4).

Potential Mechanisms of Cerebral Metabolic Stabilization by PYR

During severe decreases in perfusion beyond the range of autoregulation, glycolysis becomes an important source of ATP due to the decrease in mitochondrial oxidative phosphorylation. However, the accumulation of lactate, reduced nicotinamide adenine dinucleotide (NADH), and H^+ ions may eventually inhibit glycolysis at the level of glyceraldehyde-3-phosphate dehydrogenate (GAPDH). The continued consumption of high-energy phosphates results in depletion of the PCr and ATP pools and a concomitant a rise in extracellular Ado, Ino, and HX (44). If severe enough, this metabolic deterioration decreases the ability to maintain cellular or ionic homeostasis, and, in the cerebral cortex, ultimately results in the release of glutamate (13, 30, 39).

In this study, the PYR-treated animals, in contrast to the HTS and NS controls, show a profile of metabolic

preservation and a near absence of glutamate release. These definitively different metabolic profiles are most likely a consequence of metabolic stabilization from the PYR infusion. Furthermore, these results are consistent with in vitro data which show that PYR can be used as a primary metabolic substrate and can prolong neuronal viability in cultures (20, 27) improve neurophysiological function in isolated nervous tissue (20), and protects neurons from death induced by H_2O_2 (12) and ischemia (27).

In this study, the neuroprotective features of PYR can possibly be attributed to its improvement of neuronal energy status (Table 3). Our microdialysis data suggest that PYR crosses the blood-brain barrier and thus is available for use by neuronal tissue to enhance metabolic stability during the prolonged hemorrhagic hypotension. Furthermore, the increased microdialysis PYR levels are consistent with the current knowledge of the monocarboxylate transport (MCT) system and alternative substrate utilization by the brain (10, 16, 17, 32). Normally, glucose is the major fuel for oxidative and glycolytic metabolism in the brain. However, during periods of decreased glucose availability, the brain can use monocarboxylates as an alternative fuel source (18). Whereas PYR can serve as the sole energy source of neuronal cells in culture, PYR utilization in vivo requires transport across the blood-brain barrier and subsequent delivery to the neurons. Because of the unique properties of the blood-brain barrier, neuronal cells are believed to be dependent on astrocytes for intercellular shuttling of metabolic substrates from the capillary endothelium to neurons. Previous studies (10, 17, 32) of in vivo PYR utilization in rats and humans show that PYR is rapidly transported across the blood-brain barrier and utilized by neuronal tissue. In addition, a recent review (16) of MCT isoforms reveals that the the Michaelis-Menten constant (K_m) for PYR transport in vascular endothelium of the blood-brain barrier is near 1 mM. Thus the 5 mM blood levels of PYR attained in this study are more than sufficient to increase PYR delivery to astrocytes for transport to neuronal tissue. However, the relatively low interstitial PYR levels (0.43 mM) compared with the arterial levels may be due either to limited transport capacity of the MCT system and/or rapid utilization of PYR by astrocytes and neurons. Although there are no available studies that completely define the use of PYR as an alternative metabolic source for the cerebral cortex in vivo, existing evidence (16) suggests that it rapidly crosses the blood-brain barrier and serves as an alternative neuronal energy and or redox substrate with a transport affinity that is 3- and 10-fold greater than for lactate or ketones, respectively.

The cerebral cortical energy-related parameters evaluated in this study could indicate that production of ATP was preserved and/or its depletion attenuated by the administration of PYR. In contrast to vessel occlusion or complete cardiac arrest, hemorrhagic shock represents a low-flow state with the limited cerebral delivery of O_2 and glucose. Thus the inability of the cerebral cortex to stabilize ATP during hemorrhagic shock could be related not only to relative substrate (O_2) deprivation but also to the limited capacity and/or inhibition of energy-yielding metabolic pathways. Within this context, the beneficial effects of the PYR treatment on cortical ATP biopsy content and the microdialysis indicators of ATP degradation is probably related to the ability of PYR to enhance ATP production through mitochondrial mechanisms and/or relief of NADH inhibition of GAPDH. There are two potential major areas where PYR could facilitate mitochondrial ATP production: *1*) the PYR dehydrogenase complex, and *2*) mitochondrial respiratory function. The PDH complex is the primary point for control of carbohydrate entry into the citric acid cycle for end oxidation. During cerebral ischemia-reperfusion, reversible inhibition occurs through phosphorylation of the PDH complex (8, 25, 36, 45). This reduces the delivery of acetyl-CoA carbon and PYR-reducing equivalents to the mitochondrial matrix for NADH production, oxidative phosphorylation, and ATP production (26, 40). However, PYR also directly increases the activity of the PDH complex by inhibiting its phosphorylation by PYR dehydrogenase kinase (25). The increased PYR levels and the enhancement of PDH activity in combination with PYR carboxylation by the mitochondrial carboxylase results in anaplerosis of the citric acid cycle and maximizes mitochondrial NADH (26). Thus the PYR-increased availability of NADH in the mitochondria (40), in conjunction with the decreased NADH in the cytosol through the L/P-induced changes in the redox potential, increases the mitochondrial transmembrane H^+ gradient. This can facilitate oxidative phosphorylation and improve the ability of the cell to adapt to changing energy demands (26, 40).

A second potential mitochondrial mechanism that could be positively affected by PYR is the reversal of peroxynitrite-mediated inhibition of mitochondrial respiratory function. In low concentrations, NO modulates mitochondrial respiration by competing for the O_2-binding site of cytochrome oxidase (4). During cerebral ischemia there is a substantial increase in nitric oxide (NO) production. Because of competitive inhibition, higher concentrations of NO result in a stronger inhibition of respiratory function with a subsequent decrease in ATP production. This inhibition is reversed only by removal of NO or by increased O_2 content (15). NO inhibition of cytochrome oxidase is effectively reduced by the reaction of NO with the superoxide anion resulting in the formation of peroxynitrite (37). However, prolonged peroxynitrite exposure can inactivate complex I-III with a further reduction in respiration (5, 7, 24). PYR has the potential to modulate peroxynitrite-induced respiratory dysfunction in two ways. The first is through decreases in the cytosolic NADH/NAD- redox couple (26, 40). This decrease in the cytosolic redox state results in a decrease in superoxide anion levels and thus peroxynitrite production (33). Second, through anaplerosis there is an increase in the Krebs cycle intermediates oxaloacetate and citrate. This results in inhibition of phosphofructokinase and shunt-

ing of glycolytic hexose moieties to the pentose phosphate shunt. This increases NADPH, which is necessary for the maintenance of reduced glutathione, the intracellular scavenger of peroxynitrite (9, 23, 43).

Other differences between the PYR-treated animals and the controls that could have had a beneficial effect on the cerebral cortical ATP content and glutamate release are the differences in systemic acidosis and cardiovascular function. PYR definitely prevented systemic acidosis from H_{90} through the end of the protocol. This difference could be secondary to the metabolic proton-scavenging effects of PYR. Alternatively, the delivery of sufficient quantities of sodium chloride can enhance systemic acidosis (38). However, the evidence to implicate systemic acidosis as a factor in the deterioration of cerebral metabolic status during decreased cerebral blood flow is limited (21, 35, 41). Indeed, recent studies (1, 11, 22) of HTS-induced hypernatremia and acidosis on cerebral outcome during ischemia and trauma provide conflicting data regarding a potential detrimental effect. However, based on this study, there was an equivalent level of hypernatremia in the PYR and HTS groups, but the association between the prevention of acidosis and maintenance of cerebral cortical metabolic status cannot be dismissed. Another potentially confounding factor is the possibility of significant differences in cerebral blood flow between the PYR and control animals secondary to the higher cardiac index in the later stages of the protocol. However, the impact of this possibility is limited because differences in cardiac function were evident only after H_{150}, which is beyond the time that differences in cerebral ATP content, glutamate release, and ECOG deterioration were observed.

In conclusion, our findings reveal a novel method of decreasing the deleterious effects of hypotension by using PYR to improve energetic and redox status of the cerebral cortex. The effect of the improved ATP stability was to minimize deterioration of electrophysiologic function and strongly attenuate neuronal glutamate release during severe hypoperfusion (Fig. 4). This decrease in glutamate release will minimize the secondary excitotoxic damage on neurons in the cerebral cortex. However, this study does not establish a threshold blood level of PYR for these beneficial effects. If the kinetics of the MCT system is the limiting factor in neuronal PYR utilization, then doses as low as 2–3 mM should also be effective. Furthermore, whereas PYR was effective in preventing ATP depletion during prolonged hypotension, the precise mechanism or combination of mechanisms remains unclear. This finding could be associated with the higher cardiac index during the last hour of the protocol. Another possibility is the PYR attenuation of the potentially detrimental effects of systemic acidosis. On a cellular basis, there is supporting evidence from previous work to suggest that PYR-induced increases in PDH activity can improve metabolic function. In addition, the theoretical advantages and relative impact of decreases in peroxynitrite generation and improved GSH scavenging are unknown. Thus the eventual decline in cortical biopsy ATP content at 4 h in the PYR group is not fully understood, but could reflect inactivation of PDH despite sustained levels of PYR and/or high levels of NO/peroxynitrite that are cytotoxic. This study provides further evidence to support the conceptual framework for metabolic substrate manipulation of cellular metabolism to minimize injury. Future studies targeted at defining the global and mitochondrial mechanisms modulating the beneficial effects of PYR will aid in the translation of these observations into increased survival and functional status after resuscitation.

This work was supported in part by the Office of Research and Development, Medical Research Service, Department of Veterans Affairs, and in part by the Division of Surgery, Walter Reed Army Institute of Research.

REFERENCES

1. **Bhardwaj A, Harukuni I, Murphy SJ, Alkayed NJ, Crain BJ, Koehler RC, Hurn PD, and Traystman RJ.** Hypertonic saline worsens infarct volume after transient focal ischemia in rats. *Stroke* 31: 1694–1701, 2000.
2. **Bickell WH, Wall MJ Jr, Pepe PE, Martin RR, Ginger VF, Allen MK, and Mattox KL.** Immediate versus delayed fluid resuscitation for hypotensive patients with penetrating torso injuries. *N Engl J Med* 331: 1105–1109, 1994.
3. **Blow O, Magliore L, Claridge JA, Butler K, and Young JS.** The golden hour and the silver day: detection and correction of occult hypoperfusion within 24 hours improves outcome from major trauma. *J Trauma* 47: 964–969, 1999.
4. **Borutaite V and Brown GC.** Rapid reduction of nitric oxide by mitochondria, and reversible inhibition of mitochondrial respiration by nitric oxide. *Biochem J* 315: 295–259, 1996.
5. **Brown GC.** Nitric oxide and mitochondrial respiration. *Biochim Biophys Acta* 1411: 351–369, 1999.
6. **Burris D, Rhee P, Kaufmann C, Pikoulis E, Austin B, Eror A, De Braux S, Guzzi L, and Leppaniemi A.** Controlled resuscitation for uncontrolled hemorrhagic shock. *J Trauma* 46: 216–223, 1999.
7. **Cassina A and Radi R.** Differential inhibitory action of nitric oxide and peroxynitrite on mitochondrial electron transport. *Arch Biochem Biophys* 328: 309–316, 1996.
8. **Chang L, Shimizu H, Abiko H, Swanson R, Faden A, James T, and Weinstein P.** Effect of dichloroacetate on recovery of brain lactate, phosphorus energy metabolites, and glutamate during reperfusion after complete cerebral ischemia in rats. *J Cereb Blood Flow Metab* 12: 1030–1038, 1992.
9. **Clementi E, Brown G, Feelisch M, and Moncada S.** Persistent inhibition of cell respiration by nitric oxide: crucial role of S-nitrosylation of mitochondrial complex I and protective action of glutathione. *Proc Natl Acad Sci USA* 95: 7631–7636, 1998.
10. **Cremer JE, Teal HM, and Cunningham VJ.** Inhibition, by 2-oxo acids that accumulate in maple-syrup-urine disease, of lactate, pyruvate, and 3-hydroxybutyrate transport across the blood-brain barrier. *J Neurochem* 39: 674–677, 1982.
11. **De Witt DS, Prough DS, Deal DD, Vines SM, and Hoen H.** Hypertonic saline does not improve cerebral oxygen delivery after head injury and mild hemorrhage in cats. *Crit Care Med* 24: 109–117, 1996.
12. **Desagher S, Glowinski J, and Premont J.** Pyruvate protects neurons against hydrogen peroxide-induced toxicity. *J Neurosci* 17: 9060–9067, 1997.
13. **Drejer J, Benveniste H, Diemer NH, and Schousboe A.** Cellular origin of ischemia-induced glutamate release from brain tissue in vivo and in vitro. *J Neurochem* 45: 145–151, 1985.
14. **Enblad P, Valtysson J, Andersson J, Lilja A, Valind S, Antoni G, Angstrom L, Hillered L, and Persson L.** Simultaneous intracerebral microdialysis and positron emission tomography in the detection of ischemia in patients with subarachnoid hemorrhage. *J Cereb Blood Flow Metab* 16: 637–644, 1996.

15. **Giuffre A, Sarti P, D'Itri E, Buse G, Soulimane T, and Brunori M.** On the mechanism of inhibition of cytochrome c oxidase by nitric oxide. *J Biol Chem* 271: 33404–33408, 1996.
16. **Halestrap AP and Price NT.** The proton-linked monocarboxylate transporter (MCT) family: structure, function and regulation. *Biochem J* 2: 281–299, 1999.
17. **Hara T, Yokoi F, and Iio M.** Brain ischemia and infarction positively visualized by pyruvate-1–11C using positron-emission tomography. *Eur J Nucl Med* 12: 21–26, 1986.
18. **Harding JE and Charlton VE.** Effect of lactate and beta-hydroxybutyrate infusions on brain metabolism in the fetal sheep. *J Dev Physiol* 14: 139–146, 1990.
19. **Horton JW and McDonald G.** Heart and brain nucleotide pools during hemorrhage and resuscitation. *Am J Physiol Heart Circ Physiol* 259: H1781–H1788, 1990.
20. **Izumi Y, Benz A, Katsuki H, and Zorumski C.** Endogenous monocarboxylates sustain hippocampal synaptic function and morphological integrity during energy deprivation. *J Neurosci* 17: 9448–9457, 1997.
21. **Katsura K, Kurihara J, Siesjo BK, and Wieloch T.** Acidosis enhances translocation of protein kinase C but not Ca(2+)/calmodulin-dependent protein kinase II to cell membranes during complete cerebral ischemia. *Brain Res* 849: 119–127, 1999.
22. **Kempski O, Obert C, Mainka T, Heimann A, and Strecker U.** "Small volume resuscitation" as treatment of cerebral blood flow disturbances and increased ICP in trauma and ischemia. *Acta Neurochir Suppl (Wien)* 66: 114–117, 1996.
23. **Le Goffe C, Vallette G, Jarry A, Bou-Hanna C, and Laboisse CL.** The in vitro manipulation of carbohydrate metabolism: a new strategy for deciphering the cellular defence mechanisms against nitric oxide attack. *Biochem J* 3: 643–648, 1999.
24. **Lizasoain I, Moro M, Knowles R, Darley-Usmar V, and Moncada S.** Nitric oxide and peroxynitrite exert distinct effects on mitochondrial respiration which are differentially blocked by glutathione or glucose. *Biochem J* 314: 877–880, 1996.
25. **Lyn D and Coore HG.** Pyruvate inhibition of pyruvate dehydrogenase kinase is a physiological variable. *Biochem Biophys Res Commun* 126: 992–998, 1985.
26. **Mallet RT and Sun J.** Mitochondrial metabolism of pyruvate is required for its enhancement of cardiac function and energetics. *Cardiovasc Res* 42: 149–161, 1999.
27. **Matsumoto K, Yamada K, Kohmura E, Kinoshita A, and Hayakawa T.** Role of pyruvate in ischaemia-like conditions on cultured neurons. *Neurol Res* 16: 460–464, 1994.
28. **Melani A, Pantoni L, Corsi C, Bianchi L, Monopoli A, Bertorelli R, Pepeu G, and Pedata F.** Striatal outflow of adenosine, excitatory amino acids, gamma-aminobutyric acid, and taurine in awake freely moving rats after middle cerebral artery occlusion: correlations with neurological deficit and histopathological damage. *Stroke* 30: 2448–2455, 1999.
29. **Meldrum BS and Brierley JB.** Brain damage in the rhesus monkey resulting from profound arterial hypotension. II. Changes in the spontaneous and evoked electrical activity of the neocortex. *Brain Res* 13: 101–118, 1969.
30. **Mendelowitsch A, Sekhar LN, Wright DC, Nadel A, Miyashita H, Richardson R, Kent M, and Shuaib A.** An increase in extracellular glutamate is a sensitive method of detecting ischaemic neuronal damage during cranial base and cerebrovascular surgery. An in vivo microdialysis study. *Acta Neurochir (Wien)* 140: 349–356, 1998.
31. **Miller, AT Jr, Shen AL, and Bonner FB.** Hemorrhagic shock in the rat: metabolic changes in brain and liver. *Arch Int Physiol Biochim Biophys* 82: 69–74, 1974.
32. **Miller LP and Oldendorf WH.** Regional kinetic constants for blood-brain barrier pyruvic acid transport in conscious rats by the monocarboxylic acid carrier. *J Neurochem* 46: 1412–1416, 1986.
33. **Mohazzab HKM, Kaminski PM, and Wolin MS.** Lactate and PO_2 modulate superoxide anion production in bovine cardiac myocytes: potential role of NADH oxidase. *Circulation* 96: 614–620, 1997.
34. **Mongan PD, Fontana JL, Chen R, and Bunger R.** Intravenous pyruvate prolongs survival during hemorrhagic shock in swine. *Am J Physiol Heart Circ Physiol* 277: H2253–H2263, 1999.
35. **Nagao S, Kitaoka T, Fujita K, Kuyama H, and Ohkawa M.** Effect of tris-(hydroxymethyl)-aminomethane on experimental focal cerebral ischemia. *Exp Brain Res* 111: 51–56, 1996.
36. **Peeling J, Sutherland G, Brown RA, and Curry S.** Protective effect of dichloroacetate in a rat model of forebrain ischemia. *Neurosci Lett* 208: 21–24, 1996.
37. **Poderoso JJ, Lisdero C, Schopfer F, Riobo N, Carreras MC, Cadenas E, and Boveris A.** The regulation of mitochondrial oxygen uptake by redox reactions involving nitric oxide and ubiquinol. *J Biol Chem* 274: 37709–37716, 1999.
38. **Prough DS and Bidani A.** Hyperchloremic metabolic acidosis is a predictable consequence of intraoperative infusion of 0.9% saline. *Anesthesiology* 90: 1247–1249, 1999.
39. **Rossi DJ, Oshima T, and Attwell D.** Glutamate release in severe brain ischaemia is mainly by reversed uptake. *Nature* 403: 316–321, 2000.
40. **Scholz TD, Laughlin MR, Balaban RS, Kupriyanov VV, and Heineman FW.** Effect of substrate on mitochondrial NADH, cytosolic redox state, and phosphorylated compounds in isolated hearts. *Am J Physiol Heart Circ Physiol* 268: H82–H91, 1995.
41. **Siesjo BK, Katsura KI, Kristian T, Li PA, and Siesjo P.** Molecular mechanisms of acidosis-mediated damage. *Acta Neurochir Suppl (Wien)* 66: 8–14, 1996.
42. **Soucy DM, Rude M, Hsia WC, Hagedorn FN, Illner H, and Shires GT.** The effects of varying fluid volume and rate of resuscitation during uncontrolled hemorrhage. *J Trauma* 46: 209–215, 1999.
43. **Tejero-Taldo MI, Caffrey JL, Sun J, and Mallet RT.** Antioxidant properties of pyruvate mediate its potentiation of beta-adrenergic inotropism in stunned myocardium. *J Mol Cell Cardiol* 31: 1863–1872, 1999.
44. **Valtysson J, Persson L, and Hillered L.** Extracellular ischaemia markers in repeated global ischaemia and secondary hypoxaemia monitored by microdialysis in rat brain. *Acta Neurochir (Wien)* 140: 387–395, 1998.
45. **Zaidan E, Sheu KF, and Sims NR.** The pyruvate dehydrogenase complex is partially inactivated during early recirculation following short-term forebrain ischemia in rats. *J Neurochem* 70: 233–241, 1998.